Quantum phase transition in (CuCl)La(Nb$_{1-x}$Ta$_x$)$_2$O$_7$

A. Kitada,[1] Y. Tsujimoto,[1] H. Kageyama,[1,*] Y. Ajiro,[1] M. Nishi,[2] Y. Narumi,[2] K. Kindo,[2] M. Ichihara,[2] Y. Ueda,[2] Y. J. Uemura,[3] and K. Yoshimura[1]

[1]*Department of Chemistry, Graduate School of Science, Kyoto University, Kyoto 606-8502, Japan*
[2]*Institute for Solid State Physics, University of Tokyo, Kashiwa, Chiba 277-8581, Japan*
[3]*Department of Physics, Columbia University, New York, New York 10027, USA*

We demonstrate the synthesis and magnetic properties of a quasi-two-dimensional frustrated quantum spin system (CuCl)La(Nb$_{1-x}$Ta$_x$)$_2$O$_7$. We observed persistence of the spin-singlet state in (CuCl)LaNb$_2$O$_7$ up to $x \sim 0.4$, accompanied by a slight reduction in the spin gap with increasing x. In spite of unaltered cell parameters and a preserved CuCl plane, (CuCl)LaTa$_2$O$_7$ exhibits collinear antiferromagnetic (CAF) order with $T_N \sim 7$ K as observed in (CuBr)LaNb$_2$O$_7$. In the intermediate region ($0.4 < x < 1$), we observed CAF order with a significantly reduced magnetic moment but with a nearly constant T_N, suggesting that the CAF state coexists with the spin-singlet state in agreement with recent μSR results.

I. INTRODUCTION

Phenomena driven by quantum fluctuations in the vicinity of a quantum critical point in two-dimensional (2D) systems are one of the most important topics in modern physics. Motivated by the discovery of the 2D $S=1/2$ spin correlation in high-T_c superconducting cuprates, 2D quantum spin insulators based on the square lattice and its analogs have been searched for and extensively investigated. The examples include the J_1-J_2 lattice (where J_1 and J_2 denote the nearest and next-nearest exchange constants) such as Li$_2$VO(Si, Ge)O$_4$,[1] the checkerboard lattice $A_2F_2Fe_2OQ_2$ (A=Sr and Ba; Q=S and Se),[2] the 1/5 depleted square lattice CaV$_4$O$_9$,[3] and the Shastry-Sutherland lattice SrCu$_2$(BO$_3$)$_2$.[4] Although those studies have revealed intriguing properties such as a spin-disordered state and quantized magnetization plateaus to name only a few,[3–5] there are still many open issues left unsolved and therefore further search for compounds and systematic studies are required for global understanding of quantum fluctuations in 2D systems.

(CuCl)LaNb$_2$O$_7$ is an $S=1/2$ square-lattice-based antiferromagnet, where the magnetic CuCl layers are sandwiched by nonmagnetic LaNb$_2$O$_7$ blocks (Fig. 1). This material has a spin-singlet ground state and an excitation gap of Δ_{ZF} =2.3 meV. The triplet excitations are nearly Q independent despite the apparent 2D crystal structure.[6] Furthermore, field-induced magnetic order occurs at a remarkably smaller magnetic field of $H_{c1} \sim 10$ T than that expected from Δ_{ZF}.[7–9] The loss of the tetragonal symmetry and thus the deviation from the idealized J_1-J_2 model is suggested from the nuclear magnetic resonance (NMR) studies.[9] In contrast, (CuBr)LaNb$_2$O$_7$ exhibits collinear antiferromagnetic (CAF) order at a Néel temperature of $T_N=32$ K with a propagation vector $q=(\pi, 0, \pi)$.[10] Common to the two compounds, there exist competing antiferromagnetic and ferromagnetic interactions. Recent studies on a solid solution (CuCl$_{1-y}$Br$_y$)LaNb$_2$O$_7$ have revealed magnetic order by 5%-Br substitution.[11,12] However, it is noteworthy that the Br-for-Cl substitution with different ionic radii [1.82 Å for Br$^-$ and 1.67 Å for Cl$^-$ (Ref. 13)] is subject to direct and

considerable disorder of the CuCl layer itself. Not only the ratio of superexchange constants but also chemical disorder might play a significant role in driving the phase transition.

In this paper we investigated the magnetic properties of (CuCl)La(Nb$_{1-x}$Ta$_x$)$_2$O$_7$ by means of susceptibility, pulsed high-field magnetization, and elastic/inelastic neutron scattering measurements. A crucial advantage of the Ta-for-Nb substitution over the Br-for-Cl substitution is that the magnetic CuCl plane is preserved and that pentavalent Nb and Ta ions have almost the same radius (0.64 Å).[13] The present study has been performed in parallel with the muon spin relaxation (μSR) measurements of the (CuCl$_{1-y}$Br$_y$)LaNb$_2$O$_7$ and (CuCl)La(Nb$_{1-x}$Ta$_x$)$_2$O$_7$ systems[12] by a research team involving some of the authors of the present work.

II. EXPERIMENTAL PROCEDURE

The precursor phases RbLa(Nb$_{1-x}$Ta$_x$)$_2$O$_7$ (x=0, 0.2, 0.3, 0.4, 0.6, 0.8, and 1.0) were prepared via a conventional high temperature route, using stoichiometric amounts of La$_2$O$_3$ (99.99% purity), Nb$_2$O$_5$ (99.99%), Ta$_2$O$_5$ (99.99%), and 25% molar excess of Rb$_2$CO$_3$ (99.9%). RbLa(Nb$_{1-x}$Ta$_x$)$_2$O$_7$ was then mixed with a twofold molar excess of ultradry CuCl$_2$ (99.999%) and pressed into pellets in an Ar-filled glove box ($<$1 ppm O$_2$/H$_2$O). The ion-exchange reactions expressed as

$$\text{RbLa(Nb}_{1-x}\text{Ta}_x\text{)}_2\text{O}_7 + \text{CuCl}_2$$
$$\rightarrow \text{(CuCl)La(Nb}_{1-x}\text{Ta}_x\text{)}_2\text{O}_7 + \text{RbCl} \qquad (1)$$
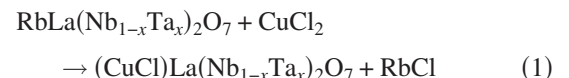
were carried out in a sealed, evacuated ($<10^{-3}$ Torr) Pyrex tube at 320 °C for seven days.[14] The final products were washed with distilled water to eliminate RbCl and excess CuCl$_2$, and dried at 120 °C.

Room temperature x-ray diffraction (XRD) profiles of (CuCl)LaNb$_2$O$_7$ and (CuCl)LaTa$_2$O$_7$ were indexed into a tetragonal cell with nearly the same lattice constants (a =3.879 Å, c=11.754 Å for Nb, and a=3.879 Å, c =11.748 Å for Ta), consistent with those previously
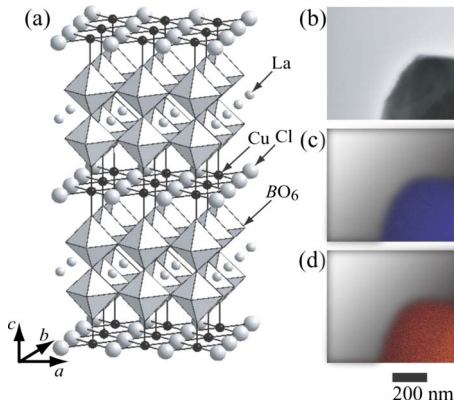
FIG. 1. (Color online) (a) Schematic view of the crystal structure of $(CuCl)LaB_2O_7$ (B=Nb, Ta). (b) TEM image and [(c) and (d)] the corresponding EDS maps of the x=0.8 sample, where blue and red dots represent Nb and Ta, respectively.

reported.[14,15] No trace of impurity phases were found. The XRD patterns of the $0 < x < 1$ samples at room temperature demonstrated successful synthesis of the solid solution having nearly the same tetragonal cell parameters as those of $(CuCl)LaNb_2O_7$ and $(CuCl)LaTa_2O_7$. The quality of the XRD patterns is as good as that of the end members. Recent NMR and transmission electron microscopy (TEM) experiments showed that the space group of $(CuCl)LaNb_2O_7$ is not $P4/mmm$; the C_4 symmetry is lost both at the Cu and Cl sites and the original unit cell is doubled along the a and b axes. Similar features might be also present in $(CuCl)LaTa_2O_7$ and the solid solution.

To check the chemical homogeneity in the solid solution system, energy-dispersive spectroscopy (EDS) was carried out at ambient temperature using a JEM2010F system with an operating voltage of 200 kV at the Institute for Solid State Physics (ISSP) at the University of Tokyo. The specimen was finely ground in methanol and then placed on a Cu microgrid mesh for TEM observations. As a typical example, we show the TEM image of the x=0.8 sample in Fig. 1(b) and the corresponding EDS spectrum in Figs. 1(c) and 1(d), which demonstrates a uniform distribution of the Nb and Ta atoms.

Magnetic susceptibilities were measured using the Quantum Design MPMS (Magnetic Property Measurement System) over the temperature range T=2–300 K in a magnetic field H of 2 T. High-field magnetization measurements up to 57 T were conducted using a pulsed magnet installed at ISSP. Elastic and inelastic neutron scattering experiments were performed using the ISSP-PONTA triple-axis spectrometer (5G), installed at the JRR-3 reactor at the Japan Atomic Energy Agency (JAEA), Tokai. Powder samples (x=0.3, 0.6, 0.8, and 1.0) of about 20 g each were put into aluminum cylinders. Neutrons with a wavelength of 2.358 Å were obtained from the 002 reflection of pyrolytic graphite (PG), and a horizontal collimation of open-40′-sample-80′-80′ in combination with a PG filter was placed before the sample to eliminate higher-order beam contamination.

III. RESULTS AND DISCUSSIONS

Shown in Fig. 2 are the magnetic susceptibilities χ for all the samples. χ of $(CuCl)LaTa_2O_7$ (x=1) above 50 K was
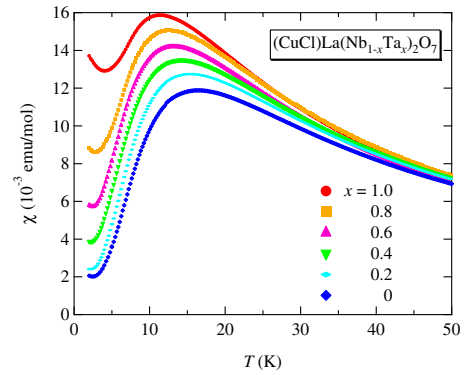

FIG. 2. (Color online) Magnetic susceptibilities of $(CuCl)La(Nb_{1-x}Ta_x)_2O_7$ measured at H=2 T.

fitted to the Curie-Weiss law, χ=$C/(T-\theta)$, where C and θ represent the Curie constant and the Weiss temperature. The value of C of 0.410 emu K/(mol Cu) suggests the completion of the designed ion-exchange reaction [Eq. (1)]. The value of θ of -1.2 K is about 1/8 of what was obtained for x=0 (-9.6 K).[6] This does not simply mean much reduced magnetic interactions because the susceptibility has a broad maximum at T_{max}^χ=11.5 K. This is a characteristic feature of low-dimensional magnetic materials, indicating that a dominant antiferromagnetic interaction is of same order of the magnitude as in x=0. The observed T_{max}^χ does not differ so much from that of x=0 (16.5 K). However, unlike χ for x=0 having a sharp drop due to spin-singlet formation, χ for x=1.0 exhibits only a slight decrease below T_{max}^χ, followed by a Curie tail, presumably due to paramagnetic impurities and defects. Thus a magnetic ground state is expected for x=1.0.
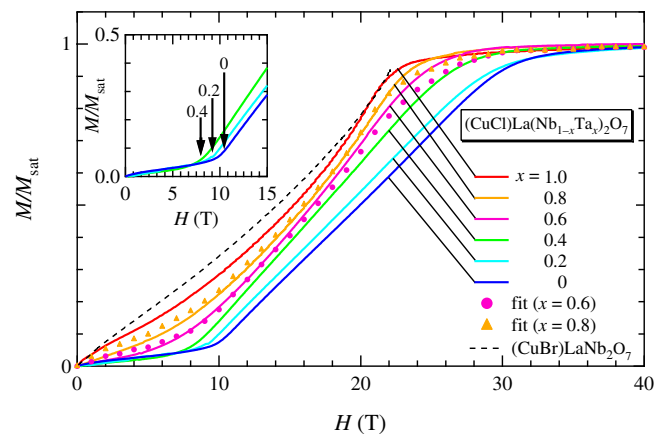

FIG. 3. (Color online) Magnetization curves M of $(CuCl)La(Nb_{1-x}Ta_x)_2O_7$ at T=1.3 K. The normalized magnetization for $(CuBr)LaNb_2O_7$ (broken line) was obtained from the data in Ref. 10 as its saturation field equals to that of x=1.0 ($\sim$23 T). Circles and triangles represent fitted curves to the x=0.6 and 0.8 data, respectively (see text for details). Inset is an enlarged plot for x=0, 0.2 and 0.4, highlighting the critical fields H_c, which were assigned to the fields of the inflection points in dM/dH. The very slow increases in magnetization below H_c are due to tiny amount of defect and/or unknown magnetic impurity as mentioned in Refs. 7 and 9.
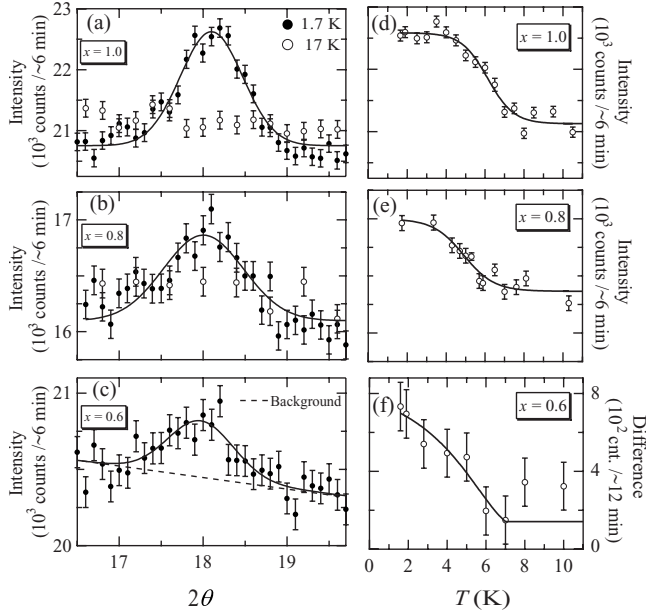
FIG. 4. [(a)–(c)] Neutron diffraction profiles of $x=1.0$, 0.8, and 0.6 around the $(\frac{1}{2}, 0, \frac{1}{2})$ magnetic reflection. Open and closed circles represent the data collected at 1.7 and 17 K, respectively, and solid lines are a guide to the eyes. A broken line in (c) represents the background. [(d)–(e)] Temperature dependence of the intensity of the $(\frac{1}{2}, 0, \frac{1}{2})$ reflection. The lines are a guide to the eyes. (f) Temperature dependence of the difference between intensity of the $(\frac{1}{2}, 0, \frac{1}{2})$ reflection and the background. The lines are a guide to the eyes.

This speculation is supported by the magnetization measurements at 1.3 K (see Fig. 3). While the magnetization curve for $x=0$ remains zero until the field-induced magnetic order occurs at H_c, apart from a tiny magnetization coming from a small amount of impurities/defects,[7,9] the magnetization curve for $x=1.0$ has a sizable slope even in low fields.

In order to probe probable magnetic order, we performed the neutron powder diffraction measurements at zero magnetic field as shown in Fig. 4(a). We found a peak at around 18° corresponding to the $(\frac{1}{2}, 0, \frac{1}{2})$ magnetic reflection. Hence, it is natural to consider that $(CuCl)LaTa_2O_7$ exhibits CAF order as in $(CuBr)LaNb_2O_7$.[10] The ordered magnetic moment was estimated to be $0.69 \pm 0.1\mu_B$, which is comparable to that of $(CuBr)LaNb_2O_7$ $(0.60 \pm 0.11\mu_B)$. However, the T dependence of the intensity of this reflection [Fig. 4(d)] revealed that the transition temperature 7 K is much smaller than that for $(CuBr)LaNb_2O_7$ (32 K). The magnetization curve for $x=1.0$ becomes very nonlinear compared with the normalized one for $(CuBr)LaNb_2O_7$ (Fig. 3), suggesting that the effect of quantum fluctuations should be considerably stronger in the former material.

We wish to recall here that the cell parameters of $(CuCl)LaTa_2O_7$ and $(CuCl)LaNb_2O_7$ are almost the same. Therefore, if the LaB_2O_7 perovksite slabs acted simply as *spacers* that spatially and magnetically isolated the CuCl layers, the magnetic properties of the two compounds would be identical. The present result indicates that superexchange interactions through Cu-BO_6-BO_6-Cu ($B=$ Nb, Ta) play an important role as well as those through Cu-X-Cu in the magnetic properties. This is compatible with the observations that the unpaired electron of Cu^{2+} ion occupies the $d(3z^2-r^2)$ orbital pointing parallel to the c axis[9] and that the stability of the 1/3 magnetization plateau in $(CuBr)A_2B_3O_{10}$ ($A=$Ca, Sr, Ba, and Pb) is tuned by substituting different atoms in the B site.[16] The cases in which $d(3z^2-r^2)$ orbitals align perpendicular to the magnetic layers is also found in the $S=1/2$ honeycomb antiferromagnet $InCu_{2/3}V_{1/3}O_3$, where superexchange interactions via InO_6 are expected to influence its magnetic properties.[17]

Once we confirmed that our two isostructural compounds had different ground states (i.e., spin-singlet and CAF states), we were able to study the magnetic phase diagram in
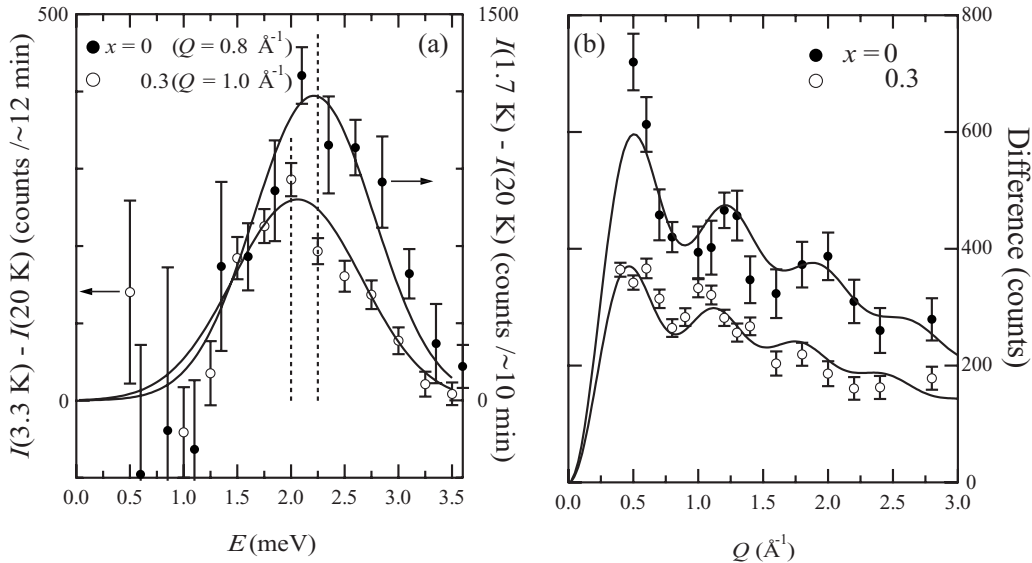

FIG. 5. Results of inelastic neutron scattering measurements for $x=0$ (closed circles) (Ref. 6) and 0.3 (open circles). (a) The difference $I(1.7\text{ K})-I(20\text{ K})$ for $x=0$ and $I(3.3\text{ K})-I(20\text{ K})$ for $x=0.3$. The curve represents a least-squares fit to a Gaussian. (b) Peak intensities of the transition from the singlet ground state to the one-triplet excited state as a function of Q obtained at $E=2.1$ meV for $x=0$ and at $E=2.0$ meV for $x=0.3$. The solid lines represent the fits according to the equation written in Ref. 6.
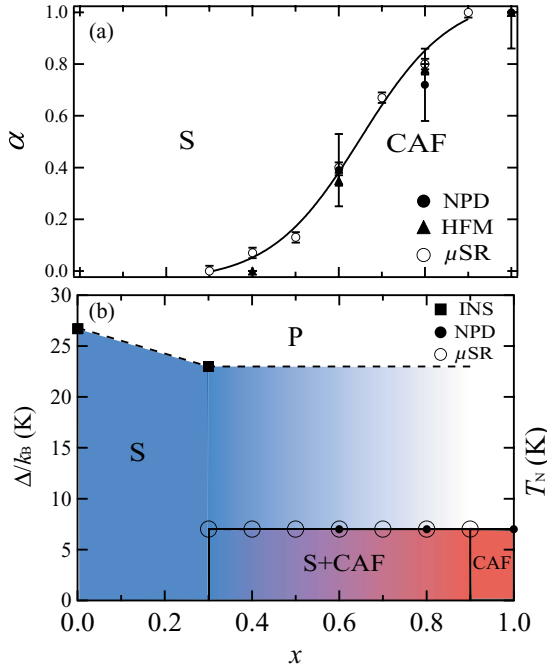
FIG. 6. (Color online) (a) Antiferromagnetic volume fraction α obtained using neutron powder diffraction (NPD) (closed circles), high-field magnetization (HFM) (closed triangles), and μSR (Ref. 12) (open circles). S stands for the spin-singlet state. The solid line is a guide to the eyes. (b) Magnetic phase diagram of $(CuCl)La(Nb_{1-x}Ta_x)_2O_7$ as a function of temperature and concentration. P stands for the paramagnetic state. Closed squares represent the zero-field gap obtained by inelastic neutron scattering (INS). S stands for the spin-singlet state. Closed and open circles denote the transition temperatures obtained by NPD and μSR (Ref. 12).

$(CuCl)La(Nb_{1-x}Ta_x)_2O_7$. Systematic evolution of the magnetic susceptibilities and the magnetization curves is shown as a function of x in Figs. 2 and 3, respectively. For example, the samples with higher x (from 0, 0.2, 0.4, 0.6, 0.8 to 1.0) have lower T^χ_{max} (16.5, 15.4, 14.2, 13.2, 12.5, and 11.5 K, respectively). The value of θ, derived from Curie-Weiss fitting to the susceptibility data, also gradually decreases with x ($\theta = -9.6, -5.6, -3.8, -3.1, -2.5$, and -1.2 K).

The M-H curves for $x=0.2$ and 0.4 trace that of $x=0$ in the low-field region, suggesting the persistence of a spin-singlet ground state. Persistent nature of the spin-singlet ground state up to 40%-Ta substitution is in marked contrast to the Cl-Br solid solution where the spin-singlet to CAF ground state transition was induced by 5%-Br substitution at most.[11,12] When the magnetic field is further increased, we found an anomaly at $H_c = 10.3, 9.1$, and 8.0 T for $x=0.0, 0.2$, and 0.4, respectively, suggestive of a field-induced phase transition. H_c decreases with x. Above H_c, the magnetization increases in proportion with H and arrives at the saturation magnetization. For $x \geq 0.4$, magnetization curves have finite slope even from low-field region, as in the case of $x=1.0$.

The energy scan at $Q=1.0$ Å^{-1} for $x=0.3$ [Fig. 5(a)] shows a singlet-triplet excitation, the peak of which is centered at $\Delta_{ZF}=2.0$ meV. This gap energy is much bigger than that expected from the high-field magnetization measure-

ments; though we have not performed magnetization measurements for $x=0.3$, H_c should be between 8.0 T ($x=0.4$) and 9.1 T ($x=0.2$) corresponding, to 0.9–1.0 meV assuming $g=2.0$. No reason has yet been given for the source of the discrepancy of the gap energy derived from neutron and magnetization measurements but the fact that there is a systematic decrease in Δ_{ZF} and H_c with x strongly suggests that it is an intrinsic property. The triplet mode is nearly Q independent, indicating the localized nature of the triplet excitations as observed in $x=0$.[6] As shown in Fig. 5(b), the Q scan result at $E=2.0$ meV for $x=0.3$ exhibits rapidly oscillating behavior similar to $x=0$. The fit to the isolated dimer model[6] yielded an unreasonably long intradimer distance of $R=9.5$ Å, implying more complex and competing magnetic interactions. Neutron powder diffraction measurements for $x=0.6$ and $x=0.8$ [Figs. 4(b) and 4(c)] show a magnetic reflection corresponding to $(\frac{1}{2}, 0, \frac{1}{2})$ indexed with respect to the chemical unit cell. Hence they should have the same spin structure as that of $x=1.0$. We also found that the ordered temperature hardly changes [Figs. 4(e) and 4(f)] while the ordered moment sizes decrease with decreasing x: $0.50 \pm 0.1 \mu_B$ ($x=0.8$) and $0.27 \pm 0.1 \mu_B$ ($x=0.6$).

Uemura *et al.*[12] recently performed μSR measurements of $(CuCl)La(Nb_{1-x}Ta_x)_2O_7$ and proposed magnetic phase separation between the static magnetic state and spin-singlet state in the range of $0.4 < x < 1.0$. This scenario requires that the magnetization curves for $x=0.6$ and 0.8 are expressed by two terms both in partial volume fractions: the spin-singlet phase (exemplified by the magnetization curve for $x=0.4$) and the CAF phase ($x=1.0$),

$$M(x) = \alpha M(1.0) + (1-\alpha)M(0.4). \quad (2)$$

In Eq. (2) α represents the volume fraction of the CAF phase and $(1-\alpha)$ represents that of the spin-singlet one. As shown in Fig. 3, the fitting curves reproduce the experimental data quite well. The obtained value of α is 0.35 for $x=0.6$ and 0.78 for $x=0.8$ which is consistent with the μSR results (0.37 for $x=0.6$ and 0.80 for $x=0.8$).[12] The decrease in intensity of the magnetic Bragg peaks can be also interpreted as a gradual decrease in the CAF partial volumes. Assuming a constant ordered moment in the CAF phase, we estimate the volume fraction $\alpha = 0.39 \pm 0.14$ for $x=0.6$ and 0.72 ± 0.15 for $x=0.8$, again consistent with the μSR results[12] and with the magnetization results presented above.

IV. CONCLUSIONS

We have demonstrated that a quantum phase transition from spin-singlet state to antiferromagnetic order occurs in $(CuCl)La(Nb_{1-x}Ta_x)_2O_7$, summarized in the magnetic phase diagram in Fig. 6(b). It is found that $(CuCl)LaTa_2O_7$ exhibits, despite the closeness of the lattice parameters in the solid solution, CAF order at $T_N \sim 7$ K. This clearly shows that the substitution of Ta^{5+} for Nb^{5+} in nonmagnetic slabs can affect the ground state of this quasi-2D magnet. The spin-singlet ground state in $(CuCl)LaNb_2O_7$ is fairly robust against Ta substitution ($0 \leq x \leq 0.4$), accompanied by a slight reduction in the spin gap, which is in marked contrast to the drastic collapse of the spin-singlet state in $(CuCl_{0.95}Br_{0.05})LaNb_2O_7$.

In the intermediate region ($0.4 < x < 1.0$), we observed CAF order but with a nearly constant T_N, likely coexisting with the spin-singlet state with systematic variation in the volume fraction [Fig. 6(a)], in agreement with the recent μSR results. This is in stark contrast to the case of $(CuCl_{1-y}Br_y)LaNb_2O_7$, where T_N increases gradually from 7 K ($y=0.05$) to 32 K ($y=1.0$).

*Author to whom correspondence should be addressed; kage@kuchem.kyoto-u.ac.jp

[1] R. Melzi, P. Carretta, A. Lascialfari, M. Mambrini, M. Troyer, P. Mittlet, and F. Mila, Phys. Rev. Lett. **85**, 1318 (2000).

[2] H. Kabbour, E. Janod, B. Corraze, M. Danot, C. Lee, M. Whangbo, and L. Cario, J. Am. Chem. Soc. **130**, 8261 (2008).

[3] K. Kodama, H. Harashina, H. Sasaki, Y. Kobayashi, M. Kasai, S. Taniguchi, Y. Yasui, M. Sato, K. Kakurai, T. Mori, and M. Nishi, J. Phys. Soc. Jpn. **66**, 793 (1997).

[4] H. Kageyama, M. Nishi, N. Aso, K. Onizuka, T. Yoshihama, K. Nukui, K. Kodama, K. Kakurai, and Y. Ueda, Phys. Rev. Lett. **84**, 5876 (2000).

[5] K. Onizuka, H. Kageyama, Y. Narumi, K. Kindo, Y. Ueda, and T. Goto, J. Phys. Soc. Jpn. **69**, 1016 (2000).

[6] H. Kageyama, T. Kitano, N. Oba, M. Nishi, S. Nagai, K. Hirota, L. Viciu, J. B. Wiley, J. Yasuda, Y. Baba, Y. Ajiro, and K. Yoshimura, J. Phys. Soc. Jpn. **74**, 1702 (2005).

[7] H. Kageyama, J. Yasuda, T. Kitano, K. Totsuka, Y. Narumi, M. Hagiwara, K. Kindo, Y. Baba, N. Oba, Y. Ajiro, and K. Yoshimura, J. Phys. Soc. Jpn. **74**, 3155 (2005).

[8] A. Kitada, Z. Hiroi, Y. Tsujimoto, T. Kitano, H. Kageyama, Y. Ajiro, and K. Yoshimura, J. Phys. Soc. Jpn. **76**, 093706 (2007).

[9] M. Yoshida, N. Ogata, M. Takigawa, J. Yamaura, M. Ichihara, T. Kitano, H. Kageyama, Y. Ajiro, and K. Yoshimura, J. Phys. Soc. Jpn. **76**, 104703 (2007).

[10] N. Oba, H. Kageyama, T. Kitano, J. Yasuda, Y. Baba, M. Nishi, K. Hirota, Y. Narumi, M. Hagiwara, K. Kindo, T. Saito, Y. Ajiro, and K. Yoshimura, J. Phys. Soc. Jpn. **75**, 113601 (2006).

[11] Y. Tsujimoto, A. Kitada, H. Kageyama, M. Nishi, Y. Narumi, K. Kindo, Y. Kiuchi, Y. Ueda, Y. J. Uemura, Y. Ajiro, and K. Yoshimura, arXiv:0907.5103v2, J. Phys. Soc. Jpn. (to be published).

[12] Y. J. Uemura, A. A. Aczel, Y. Ajiro, J. P. Carlo, T. Goko, D. A. Goldfeld, A. Kitada, G. M. Luke, G. J. MacDougall, I. G. Mihailescu, J. A. Rodriguez, P. L. Russo, A. Tanaka, Y. Tsujimoto, C. R. Wiebe, T. J. Williams, T. Yamamoto, K. Yoshimura, and H. Kageyama, preceding paper, Phys. Rev. B **80**, 174408 (2009).

[13] R. D. Shannon, Acta Crystallogr., Sect. A: Cryst. Phys., Diffr., Theor. Gen. Crystallogr. **32**, 751 (1976).

[14] T. A. Kodenkandath, J. N. Lalena, W. L. Zhou, E. E. Carpenter, C. Sangregorio, A. U. Falster, W. B. Simmons, Jr., C. J. O'Connor, and J. B. Wiley, J. Am. Chem. Soc. **121**, 10743 (1999).

[15] T. A. Kodenkandath, A. S. Kumbhar, W. L. Zhou, and J. B. Wiley, Inorg. Chem. **40**, 710 (2001).

[16] Y. Tsujimoto, H. Kageyama, Y. Baba, A. Kitada, T. Yamamoto, Y. Narumi, K. Kindo, M. Nishi, J. P. Carlo, A. A. Aczel, T. J. Williams, T. Goko, G. M. Luke, Y. J. Uemura, Y. Ueda, Y. Ajiro, and K. Yoshimura, Phys. Rev. B **78**, 214410 (2008).

[17] V. Kataev, A. Möller, U. Löw, W. Jung, N. Schittner, M. Kriener, and A. Freimuth, J. Magn. Magn. Mater. **290-291**, 310 (2005).